PAST AND FUTURES CHANGES IN THE NORTH SEA EXTREME WAVES

Sofia Caires[1], Jacco Groeneweg[2] and Andreas Sterl[3]

Past and future changes in the North Sea extreme waves are investigated in this article. Estimates obtained from non-stationary extreme value analyses, expressing the extreme value distribution parameters as functions of time and wind speed related covariates, are given. The results show that there is a significant trend of about 9 mm/yr in the current climate extremes of significant wave height and a trend of 1 mm/yr in the projections from 2001 to 2100. The characteristics of the extremes of wave period depend on whether swell or wind-sea events are considered. If both types of events are considered, the extremes are dominated by swell events and no present or future changes are identified. Considering wind-sea events only, a trend of less than 0.01s/yr in the present climate wave periods and a trend an order of magnitude smaller in the projections from 2001 to 2001 were detected.

1. Introduction

The current approach to obtain hydraulic boundary conditions for the Dutch water defences involves stationary extreme value analysis of wave conditions that are measured at offshore locations. In such approach the extreme wave climate is assumed to be stationary. However, it is believed today that climate is not stationary, as the detection of both decadal variability and long term time trends in different climate variables, reported by several authors, indicates. The past and future changes in the North Sea wave extremes have been investigated in this paper, trying to answer questions such as: Has the North Sea extreme wave climate changed in the last decades? How is it expected to change in the future?

Previous studies on the influence of climate changes on wave extremes were based only on changes in significant wave height (see e.g. Wang and Swail, 2006 and Caires et al., 2006b). For the design of coastal defences the wave period is also an important parameter. Therefore, in this study we have not only analysed changes in extremes of significant wave height (H_s) but also changes in extremes of wave period.

A problem involved in the estimation of future wave extremes is that no projections of future wave conditions are available in the global climate model computations (IPCC 2007). Using the available global climate model results, two approaches could in principle be used to quantify future changes in the wave extremes:

- Dynamically, by using climate models wind speed projections to force a

[1] Hydraulic Engineering, Deltares | Delft Hydraulics, P.O. Box 177, 2600 MH Delft, The Netherlands, sofia.caires@deltares.nl

[2] Hydraulic Engineering, Deltares | Delft Hydraulics, P.O. Box 177, 2600 MH Delft, The Netherlands, jacco.groeneweg@deltares.nl

[3] Global Climate, Royal Netherlands Meteorological Institute (KNMI), P.O. Box 201, 3730 AE De Bilt, The Netherlands, sterl@knmi.nl

wave model and then carry out a (non-stationary) extreme value analysis of the projected timeseries.

- Statistically, by determining the dependence of the parameters of a non-stationary extreme value distribution on covariates and then using such dependences and the climate projection data to directly compute the changes in extremes.

Both approaches were considered by Wang et al. (2007) for the North Atlantic and it was concluded that, given the coarse resolution with which global climate models are presently run, the statistical approach provides more accurate results.

When in addition to the global climate model results a regional climate model is also available, another approach is to run the regional climate model using the global climate model results as boundary conditions and use the winds resulting from the regional climate model results to force a wave model. Such approach has been considered by Grabemann and Weisse (2008).

The statistical approach mentioned above will be used in this study. Quantitative results are to be presented, but the study is in essence illustrative. It is the authors' opinion that it is not only important to raise the awareness of the effects of wave climate changes in coastal engineering, but also to establish methodologies that can quantify such effects.

Caires et al. (2006a) have shown that the usual approach of estimating nearshore extreme storms by translating offshore extreme storms with an associated return period to nearshore is conservative. The approach by which the entire offshore timeseries are translated to nearshore and the resulting nearshore timeseries subsequently analysed for extreme values is preferable. Therefore, as a first step in this study, we have created a long-term wave data set (1957-2002) for a strip of the Dutch coast by running the wave model SWAN (Simulation of Waves in Nearshore Areas, Booij et al. 1999) in non-stationary mode and using the ERA-40 data (European reanalysis data set, Uppala et al., 2005) as boundary conditions. The hindcasted nearshore wave timeseries in front of the Dutch Petten sea defence (see the MP1 location in Figure 1) are subsequently analysed by using both stationary and non-stationary extreme value theory.

Using climate projections of the wind speed and the dependence of the parameters of non-stationary extreme value distribution on wind related covariates, we have determined projections of changes in return value estimates of H_s and wave period up to the end of the 21st century. The wind projections used are obtained from the ESSENCE project (http://www.knmi.nl/~sterl/Essence/); a 17-member ensemble simulation from 1950 till 2100. During the historical period (1950-2000) they are forced by observed concentrations of greenhouse gases and anthropogenic aerosols. For the future the forcing follows the SRES A1b scenario (described as: a "Balanced" progress across all resources and technologies from energy supply to end use, and considered to be one of the most realistic futures emission scenarios).

In the following sections we shall present the extreme value theory used to perform stationary and non-stationary extreme value analysis of the data; describe the creation of the long-term wave dataset; describe and present the results. We end with a discussion of the results and with conclusions.

2.

Extreme value theory

One of the currently most used methods in stationary extreme value analyses is the peaks-over-threshold (POT) method, in which the occurrence of 'storms' above a certain threshold and the magnitude of peak observations from 'independent' storms are modelled with Poisson and Generalized Pareto (GPD) distributions, respectively (see e.g. Coles 2001).

More precisely, in the POT method, the peak excesses over a high threshold u of a timeseries are assumed to occur according to a Poisson process with rate λ_u and to be independently distributed with a GPD, whose distribution function is given by

$$F_u(x) = 1 - \left(1 + \xi x / \sigma\right)^{-1/\xi}, \tag{1}$$

where $x > 0$, $\sigma > 0$ and $- \quad < \xi < \quad$. The two parameters of the GPD are called the *scale* (σ) and *shape* (ξ) parameters. For $\xi = 0$ the GPD is said to have a type I tail and it is the exponential distribution with mean σ, for $\xi > 0$ has a type II tail and it is the Pareto distribution, and for $\xi < 0$ has a type III tail and it is a special case of the beta distribution.

The 1/m-yr return value based on a POT/GPD analysis, z_m, is given by

$$z_m = \begin{cases} u - \dfrac{\sigma}{\kappa}\{\, (\lambda_u m)^{\xi} - 1 \,\}, & \text{for } \xi \quad 0 \\ u - \sigma \log(\lambda_u m), & \text{for } \xi = 0. \end{cases} \tag{2}$$

In choosing the threshold there is a trade off between bias and variance: Too low a threshold is likely to violate the asymptotic basis of the model, leading to bias; too high a threshold will generate fewer excesses with which to estimate the model, leading to high variance. An important property of the POT/GPD approach is the threshold stability property: if a GPD is a reasonable model for excesses of a threshold u_0, then for a higher threshold u a GPD should also apply; the two GPD's have identical shape parameter and their scale parameters are related by $\sigma_u = \sigma_{u_0} + \xi(u - u_0)$, which can be reparameterized as $\sigma^* = \sigma_u + \xi u$.

Consequently, if u_0 is a valid threshold for excesses to follow the GPD then estimates of both σ^* and ξ, hence the quantile estimate itself, should remain nearly constant above u_0. This property of the GPD can be used to find the minimum threshold at which a GPD model applies to the data.

The non-stationary analog of the POT/GPD approach is the non-homogeneous Poisson process (NPP). In the point process approach to modelling extreme values (Smith 1989), one looks at the times at which "high values" occur and at their magnitude. If t denotes the generic time at which a high value occurs and if x is the corresponding magnitude of the variable of interest, then the point process consists of a collection of points (t, x) in a region of the positive quadrant of the plane. Thus our point process, or rather its "realization", consists of a collection of points belonging to the plane set $C=\{(t,x): x>u, 0 \le t \le T\}$ where T is the number of years (in our case) over which observations are available and u denotes the threshold at time t. The non-homogeneous Poisson process (NPP) model of extremes is specified by the following two properties. Firstly, if A is a subset of C, then the number of points occurring in A, which we denote by N(A), is a random variable with a Poisson probability function with mean $\rho(A)$, where, writing $x_+ = \max(0,x)$ for real *x*,

$$\rho(A) = \int_A \lambda(t,x)\,dt\,dx \,, \tag{3}$$

$$\lambda(t,x) = \frac{1}{\sigma(t)}\left(1+\xi(t)\,\frac{x-\mu(t)}{\sigma(t)}\right)_+^{-\frac{1}{\xi(t)}-1} \quad \text{for } (t,x)\in C\,, \tag{4}$$

and $\mu(t)$, $\sigma(t)$ and $\xi(t)$ are respectively the *location, scale and shape parameters* - or rather “parameter functions” - that may depend on time and need to be specified and estimated in practice.

The $1/m$-yr return value, x_m, is determined by solving $\int_0^m \left(1+\xi(t)\,\frac{x_m-\mu(t)}{\sigma(t)}\right)^{-\frac{1}{\xi(t)}} dt = 1$.

In order to incorporate non-stationarity into the process we shall consider the following models for its parameters:

$$\mu(t)=\mu_0+\mu_1 P(t)+\mu_2 G(t)\,,\ \sigma(t)=\sigma_0+\sigma_1 P(t)+\sigma_2 G(t) \text{ and } \xi(t)=\xi\,, \tag{5}$$

t=1,2,...,T, where μ_1, μ_2, etc., are constants and *P(t)* and *G(t)* are covariates, i.e., observations from a timeseries which for each time *t* are to a certain degree related to the peak *x* occurring at *t*.

The parameters of the NPP (and the GPD) model outlined above are estimated by the maximum likelihood method (ML). The uncertainties are to be obtained using the profile likelihood method (Coles 2001), which is based on the deviance function and yields asymmetric confidence intervals.

In order to assess whether the dependence of the NPP location and scale parameters on the time covariates are statistically significant, we use the likelihood ratio test (Coles 2001).

In the case of the NPP model the choice of the threshold is less obvious than in the POT/GPD approach, where some experience and empirical rules exist. We will therefore, in the non-stationary extreme value analysis, use the same threshold defined in the stationary extreme value analysis.

The data sampling follows the usual POT approach, with the peak exceedances and the times at which they occur being represented by $\{t_{i,j}, x_{i,j}\}$, $j=1,2,\ldots,n_i$, $i=1,2,\ldots,T$, where n_i is the number of clusters in the *i*-

th year. They correspond to the peaks of cluster exceedences above the threshold u and the times at which they occur obtained from the 6-hourly timeseries of the hindcast data at MP1. The declustering method we use in order to arrive at this sample is the usual one of identifying clusters and picking their maxima and times where they occur. We have taken care in treating cluster maxima at a distance of less than 48 h apart as belonging to the same cluster (storm) and hence collecting only the highest of the two.

3. Data description

The ERA-40 data, which is freely available for scientific purposes, includes 6-hourly fields of wind speed at 10 meters height (U_{10}) and wave parameters, such as H_s (i.e. H_{m0}), mean zero-upcrossing wave period and mean wave direction on a global 1.5º x 1.5º latitude/longitude grid (covering thus also the North Sea) from September 1957 to August 2002. However, given its resolution and the fact that no shallow water effects are accounted for in the ERA-40 wave model, a finer resolution shallow water have model needs to be used in order to transfer the ERA-40 offshore information to our location of interest, MP1, nearshore; see Fig. 1. The shallow waters wave model SWAN was used in non-stationary mode to produce a timeseries of nearshore long-term wave conditions at MP1 from 1958 to 2001.

Figure 1 shows the locations of the ERA-40 grid points surrounding the Petten region and the nearshore Petten buoy (MP1). Figure 2 shows the region covered by the SWAN grid and the corresponding bathymetry. The grid on which the bathymetry is given coincides with the computational grid.

The model was run using the same calibration of the ERA-40 data and model settings as described in Caires et al. (2006) except for two improvements:

1. In order to improve the accuracy of the hindcasts in general a more refined time step of 20-min instead of 1 hour was used.
2. In order to improve the wave period hindcasts, which were underestimated in the previous study, the wind growth and whitecapping dissipation formulation, as recommended by Rogers et al. (2003), was used in place of SWAN's default (WAM3) formulation (Booij et al. 2007).

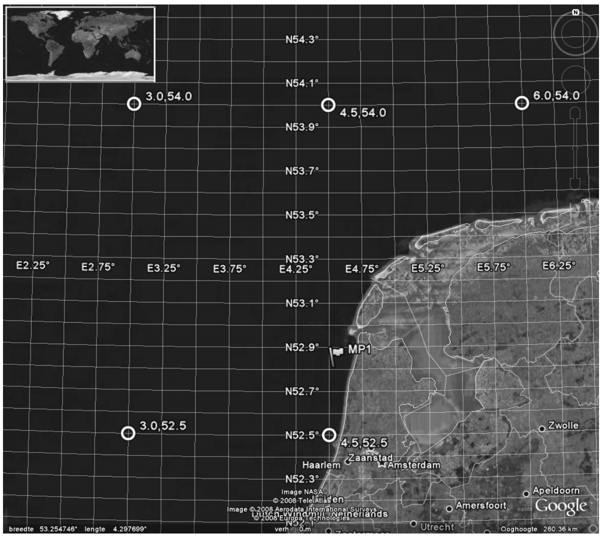

Figure 1. Google Earth aerial view of the Petten region. The white circles indicate the location of the ERA-40 gridpoints. The location of the nearshore MP1 location is flagged.

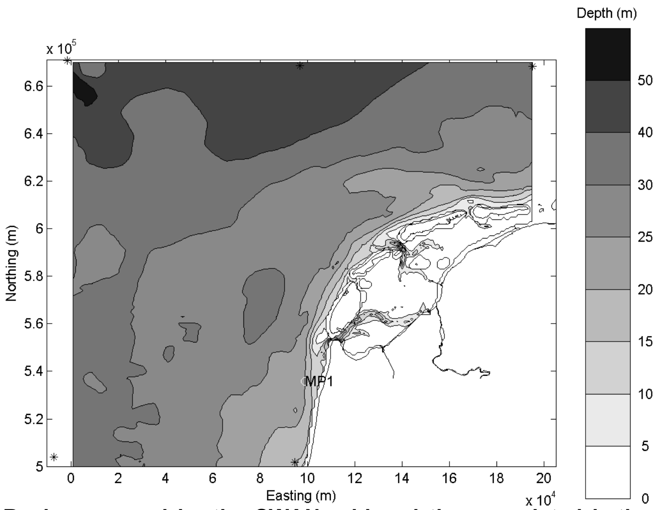

Figure 2. Region covered by the SWAN grid and the associated bathymetry. The asterisks indicate the ERA-40 grid point locations.

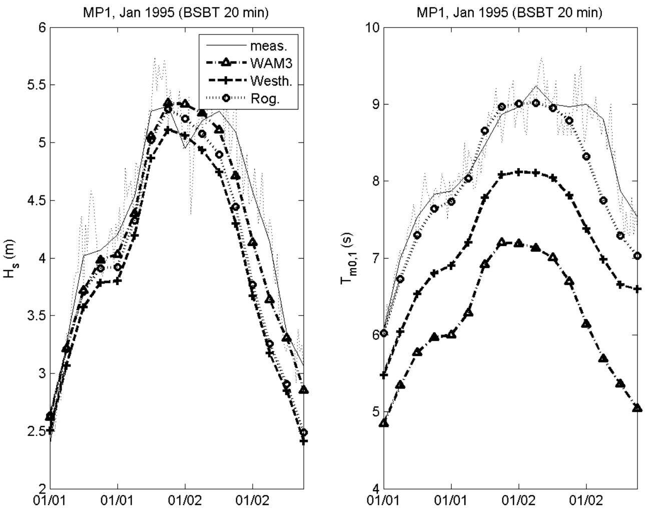

Figure 3. MP1 measurements of the January 1995 storm (light full and dashed lines) and the corresponding SWAN hindcasts using the WAM3 (triangles connected with a thick dashed-dotted line), Westh. (crosses connected with a thick dashed line) and Rog. (circles connected with a thick dotted line) configurations.

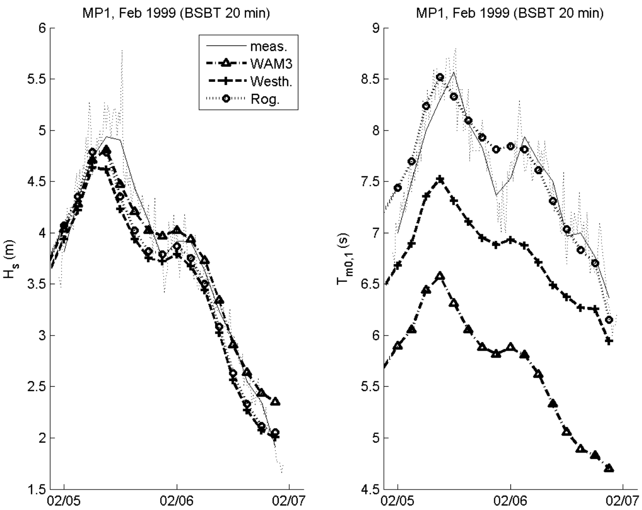

Figure 4. The same as Figure 3, but for the February 1999 storm.

Figures 3 and 4 show measurements at MP1 and SWAN hindcasts for a storm in 1995 and 1999, respectively. The hindcasts shown were computed using three wave growth and dissipation configurations in SWAN:

1. SWAN's default *WAM3* formulation;
2. the recently implemented *Westh* configuration (Westhuysen 2007), an improved version of the implementation considered in Caires et

al. 2006;

3. and the configuration recommended in Rogers et al. (2003), hereafter named the *Rog* configuration.

The figures show that all three configurations produce H_s hindcasts that compare rather well with the measurements; the hindcasts using the WAM3 configuration reproducing just slightly better the measurements. In terms of mean wave period, the hindcast using the wind growth and whitecapping settings recommended by Rogers et al. (2003) clearly reproduce the measurements better. Given that in this study we would also like to analyse wave period data, we have carried out the 44-year hindcasts using the Rog configuration.

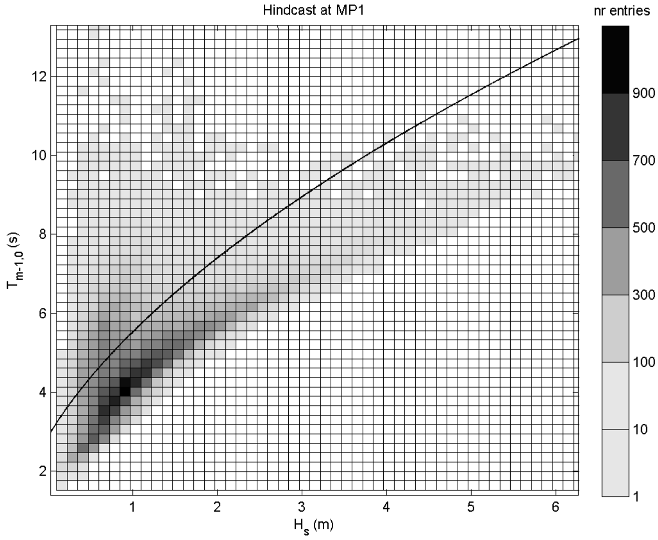

Figure 5. Density scatter of the hindcast 44-yr H_s and $T_{m-1,0}$ data. The full line crudely separates wind-sea from swell events.

Figure 5 shows the density scatter of the 44-yr H_s and $T_{m-1,0}$[4] data at MP1. The figure shows that the wave conditions nearshore the Petten Sea Defence are characterized by both swell (which here we define as wave events with long periods and low wave heights that occur mainly outside storm periods) and wind-sea events. To perform the extreme value analysis a crude separation of wind-sea and swell was used with the events for which $T_{m-1,0}$ exceeds $(H_s/4.5)^{1.8}+0.45$ being defined as swell events (cf. black line in Figure 5).

[4] The wave period $T_{m-1,0}$ is since the work of Van Gent (1999, 2001) used widely as the characteristic wave period when describing the influence of wave energy in process related to water defences and is therefore the period parameter being considered in this study.

4. Data analysis

4.1 Stationary analysis

We begin by presenting the results of the stationary extreme value analysis. We have used the threshold stability property mentioned above to choose the most appropriate threshold for selecting a sample of peak excesses and fitting the GPD to it. The chosen threshold, model parameter and 1/100-yr return values estimates are given in Table 1. The estimates were obtained with the whole H_s data, $T_{m-1,0}$ considering just wind-sea data and the whole $T_{m-1,0}$ data, respectively. It is worth mentioning that when considering the whole H_s data set the extremes are dominated by wind-sea events while when considering the whole $T_{m-1,0}$ data set the extreme are dominated by swell events. Note that in Table 1 the shape parameter estimate for the H_s data is negative, suggesting a Type III tail; this is consistent with the fact that waves in this location are in principle depth-limited, and in contrast to the Type I tail behaviour typically observed in deep waters (Caires and Sterl 2005). For $T_{m-1,0}$ data the estimates suggest that the wind-sea data have a Type III tail, i.e. that $T_{m-1,0}$ at the peaks of the win-sea storms has an upper bound. This is in contrast to the tail characteristics of the whole (i.e. including swell events as well) $T_{m-1,0}$ population.

Table 1. Parameter estimates and associated 95% confidence intervals of the GPD model fitted to the POT data

Variable	Sample size	u	λ	$\hat{\xi}$	$\hat{\sigma}$	$\hat{z}_{100}$
H_s (all)	198	3.89	4.50	-0.20 (-0.31,-0.08)	0.74 (0.60, 0.89)	6.51 (6.21,7.42)
$T_{m-1,0}$ (wind-sea)	278	7.71	6.32	-0.13 (-0.24, -0.01)	0.81 (0.67, 0.98)	11.25 (10.68, 12.54)
$T_{m-1,0}$ (swell)	185	8.58	4.20	-0.01 (-0.15, 0.13)	0.82 (0.66, 0.99)	13.37 (12.50, 15.95)

4.2 Non-stationary analysis

In order to look for trends or other systematic temporal variations of H_s and $T_{m-1,0}$ in the last decades at MP1, we have analyzed the hindcast timeseries using a non-stationary extreme value approach. We have chosen time (t) and its square (t^2) as covariates, i.e., $P(t)=t$ and $G(t)=t^2$ in (5). Note that the influence of these covariates may be felt in the form of shifts (μ_1 and/or μ_2 0) and/or changes in spread (σ_1 and/or σ_2 0) in the distribution of extremes, which can be interpreted as increases/decreases in severity and/or variability in extreme wave systems, respectively.

As regards the dependence of the parameters on the covariates, the results of the likelihood ratio tests show that for the whole $T_{m-1,0}$ data there are no significant correlations and that for the H_s and for the wind-sea $T_{m-1,0}$ data the location parameter is significantly correlated with t and not with t^2, and that the scale parameter is not significantly correlated with either t or t^2. Thus, time influences the distribution of extremes in the form of shifts (linear trend) but not in the form of changes in spread. Specifically, the changes are in the form of a linear trend of about 9 mm/yr and less than 0.01s/yr in the location parameter of the extreme value distribution of H_s and wind-sea $T_{m-1,0}$, respectively. However, the resulting changes in the 1/100-yr return value estimates are well within the 95% confidence interval of the estimate obtained from the stationary extreme value analysis. Figure 6 compares the time dependent NNP 1/100-yr return value estimate with the estimate obtained from the stationary extreme value analysis.

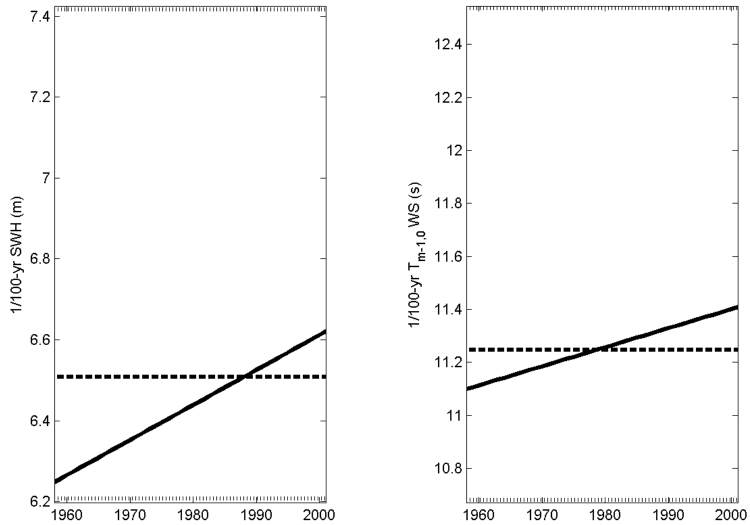

Figure 6. Stationary estimates (dashed line) and corresponding 95% confidence intervals (dotted lines) and non-stationary 1/100-yr return value estimates (full line) based on the 44-year timeseries of H_s (left panel) and wind $T_{m-1,0}$ (right panel) hindcasts at MP1.

In order to look for trends in the future H_s and $T_{m-1,0}$ extremes at MP1, we have analyzed the hindcast timeseries using the non-stationary extreme value approach. We have chosen the U_{10} and the U_{10} square monthly mean anomalies relative to the ERA-40 1971-2000 baseline climate as covariates: $P(t)$ and $G(t)$ in (5). The results of the likelihood ratio tests show that the location parameter is significantly correlated with both P and G, and that the scale parameter is not significantly correlated with either P or G. Having adopted the model $\mu(t) = \mu_0 + \mu_1 P(t) + \mu_2 G(t)$, $\sigma(t) = \sigma_0$ and $\xi(t) = \xi$ to describe the NPP parameters in terms of the wind speed covariates, and having estimated its coefficients, we have further assumed that the fitted model in each case is also valid under the future climate scenario A1b. We have therefore computed projections of the location parameter and of the 1/100-yr return values from 2001 to 2100 based on each ensemble member using the projections of P and G, obtaining a total of 17 time series of projections (one for each ensemble member) for each variable non-stationary model of extremes. Next, we have analysed the time variability of the projected series of the location parameter from 2001 to 2100 for each variable and tested whether linear or quadratic trends were present in the projections.

Similarly to the present climate estimation, no trends were found in the projections of the $T_{m-1,0}$ extremes which include the swell events. Linear trends were found to be significantly different from zero at the 5% level for both the H_s and wind-sea $T_{m-1,0}$ data. In the case of H_s the trend is of 1 mm/yr and for wind-sea $T_{m-1,0}$ data of 0.001 s/yr. Figure 7 shows the projections of H_s and wind-sea $T_{m-1,0}$ 1/100-yr return values.

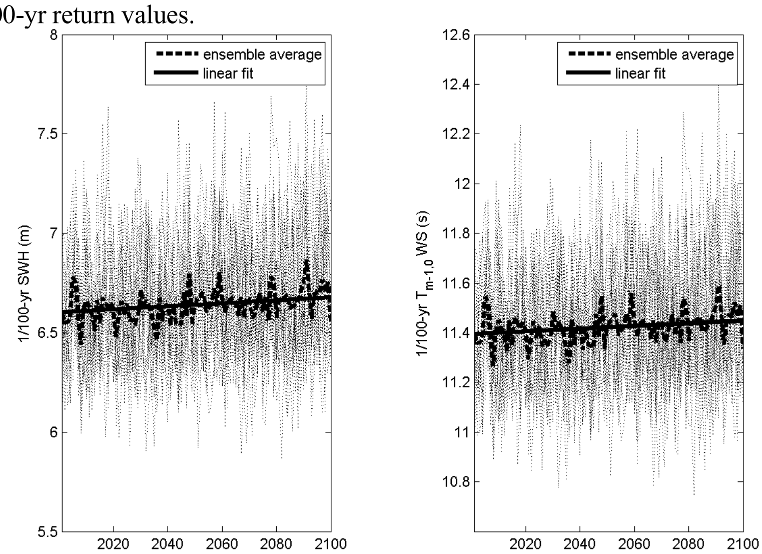

Figure 7. Projections of the H_s (left panel) and wind-sea $T_{m-1,0}$ (right panel) 1/100-yr return values.

5. Discussion and conclusions

Past and future changes in the North Sea extreme waves were investigated in this study. The results can be summarized as follows:

- The nearshore significant wave height data indicate a type III tail.
- There is a significant trend in the current climate (1958-2001) extremes of H_s of about 9 mm/yr and a trend in the projections from 2001 to 2100 of 1 mm/yr.
- The characteristics of the wave period extremes depend on whether swell or wind-sea events are considered. Considering only wind-sea events, the data indicate a type III tail. Considering also the swell events the data indicate a type I tail.
- If both types of events are considered, the extremes are dominated by swell events and no present or future changes are identified.
- Considering wind-sea events alone, a trend of less than 0.01s/yr in the present climate wave periods and a trend an order of magnitude smaller in the projections from 2001 to 2100 were detected.

There are several uncertainties associated with the future trend estimates presented here that are not accounted for in the statistical uncertainty estimated here. Firstly, only one climate scenario was considered. Secondly, this study is based on wind speed projections from only one climate model. Both scenario and climate model uncertainties are known to be large. Furthermore, the covariates chosen are monthly mean anomalies; in order to improve non-stationary extreme value fits, covariates that are more closely related to the considered extremes need to be used. However, that can only be done when the reliability of wind higher percentiles from global climate model results is known.

ACKNOWLEDGMENTS

The financial contribution by Delft Cluster through the project "Natural hazards; Loads and strength of flood defence systems; Sea defences" is acknowledged.

REFERENCES

Booij, N., R. C. Ris, and L. H. Holthuijsen. 1999. A third-generation wave model for coastal regions, Part 1: Model description and validation, J. Geophys. Res., 104(C4), 7649– 7666.

Booij, N., IJ.G. Haagsma, L.H. Holthuijsen, A.T.M.M. Kieftenburg, R.C. Ris, A.J. van der Westhuysen and M. Zijlema. 2007. SWAN Cycle III Version 40.51 Users Manual, Delft University of Technology.

Caires, S., J. Groeneweg, and A. Sterl. 2006a. Changes in North Sea extreme waves, Proc. of the 9th int. workshop on wave hindcasting and forecasting, JCOMM Tech. Rep. No. 34 / WMO-TD. No. 1368.

Caires, S. and A. Sterl. 2005. 100-year return value estimates for ocean wind speed and significant wave height from the ERA-40 data, *J. Clim.*, 18, 1032-1048

Caires, S., V. Swail and X. L. Wang, 2006b. Projection and Analysis of Extreme Wave Climate. J. Climate, 19(21), 5581-5605.

Coles, S.. 2001. An Introduction to the Statistical Modelling of Extreme Values, Springer Texts in Statistics, Springer-Verlag: London

Grabemann, I. and R. Weisse. 2008. Climate change impact on extreme wave conditions in the North Sea: An ensemble study. Ocean Dynamics, in press.

IPCC. 2007. Climate Change 2007: The Fourth Assessment Report of the Intergovernmental Panel on Climate Change; Summary for Policymakers, http://www.ipcc.ch/SPM2feb07.pdf.

Rogers, W.E., P.A. Hwang, and D.W. Wang. 2003. Investigation of wave growth and decay in the SWAN model: three regional-scale applications, *J. Phys. Oceanogr.*, 33, 366-389.

Smith, R. L. 1989. Extreme value analysis of environmental time series: an application to trend detection in ground level ozone (with discussion). *Statist. Sci.*, 4, 367-393.

Uppala, S.M., and Coauthors. 2005. The ERA-40 Reanalysis, *Quart. J. Royal Meteorol. Soc.*, 131(612), 2961-3012.

Van Gent, M.R.A. 1999. *Wave run-up and wave overtopping for double-peaked wave energy spectra*. WL | Delft Hydraulics report H3351 (see also reports H3129 and H3608), Delft, The Netherlands.

Van Gent, M.R.A.. 2001. Wave run-up on dikes with shallow foreshores. *J. of Waterways, Port, Coastal and Ocean Eng.*, ASCE, September/October 2001 issue.

Van der Westhuysen, A. J. 2007. *Advances in the spectral modelling of wind waves in the nearshore*, Ph.D. Thesis, Technical report, Fac. of Civil Engineering, Delft University of Technology.

Wang, X. L. and V. Swail, 2006. Climate change signal and uncertainty in projections of ocean wave height, *Climate Dyn.*, 26, 109-126.

Wang, X. L., V. Swail and A. Cox. 2007. Dynamical Versus Statistical Downscaling Approaches for Projecting Ocean Wave Heights, *Proc. of the 10th int. workshop on wave hindcasting and forecasting & Coastal Hazard Assessment*, JCOMM Tech. Rep. No. 44 / WMO-TD. No. 1442.

KEYWORDS – ICCE 2008

PAPER TITLE: Past and futures changes in the North Sea extreme waves

Authors: Sofia Caires, Jacco Groeneweg and Andreas Sterl
Abstract number: 462

Climate Change
North Sea
Extreme value analysis
Coastal defense
Long Term Wave Hindcast
Nearshore waves
Wave Climate